

利用W波相逆推震源參數與單位海嘯建立南中國海海嘯預警系統

交通部中央氣象局地震測報中心

陳伯飛 助理教授/國立中央大學地球科學系

1. Introduction

It is not beyond the realm of possibility that a mega-earthquake occurs in the Manila subduction zone, triggering widespread tsunamis across the South China Sea (SCS). Historical tsunami hazards on southwest coasts of Taiwan (Fig. 1) may also be caused by such SCS tsunamis, amplified by shoaling of continental shelf when approaching Taiwan. In this study, we propose to build a warning system in Taiwan for SCS tsunamis, through a combination of *W* phase inversion and unit tsunami methods.

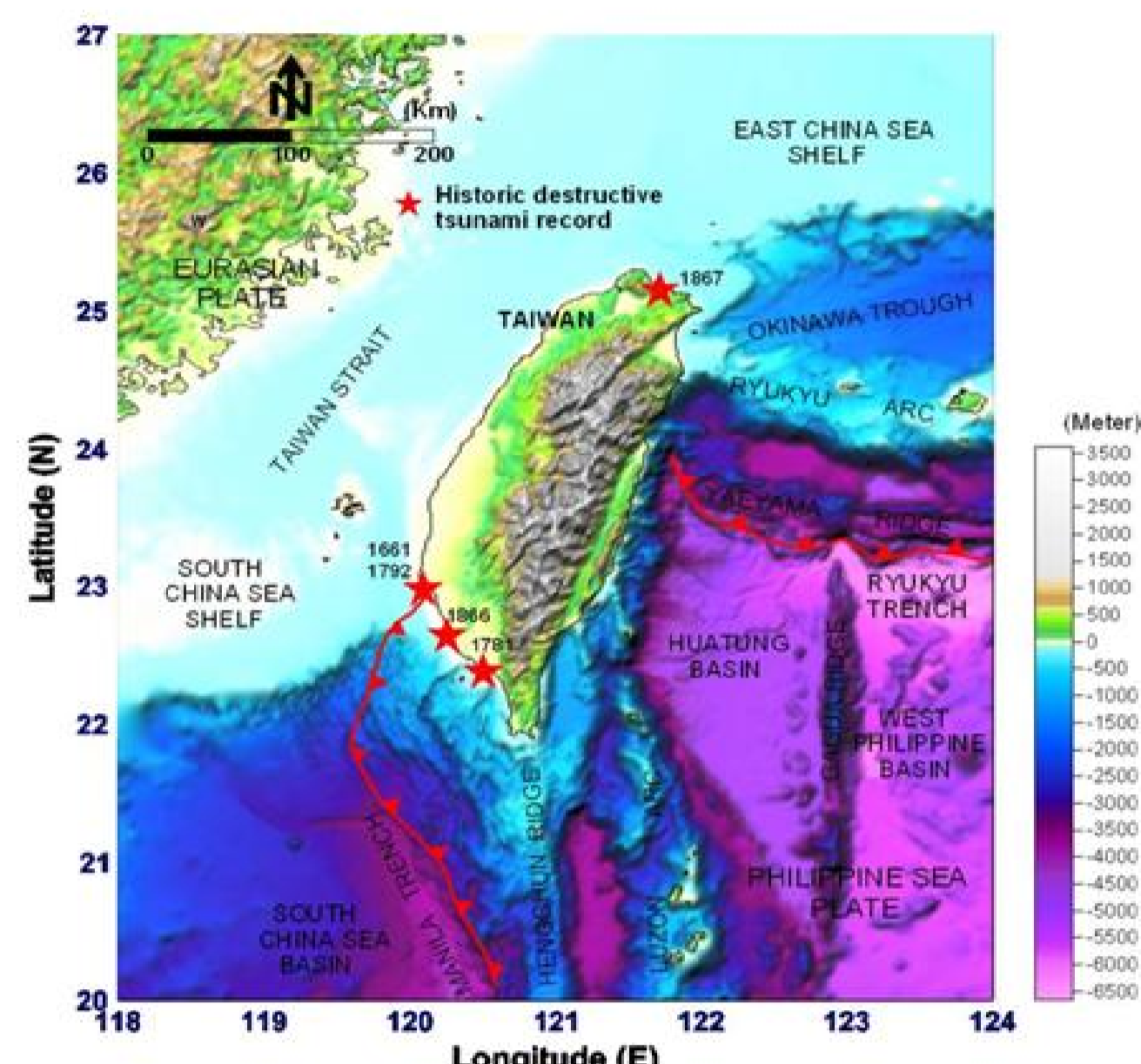


Fig. 1. Locations of historical tsunami hazards in Taiwan. Note the most distribute on North and SW Taiwan [1].

2. Data and Methods

2.1. W Phase Inversion

We refer readers to Kanamori & Rivera [2] regarding theory, modeling, and source inversion of *W* phase. We sorted out earthquakes from the GCMT catalog ([3], [4]) that occurred between January 2000 and July 2009, were bounded by 10°N/26°N and 115°E/135°E, and had moments greater than 10^{25} dyn-cm, (Fig. 2). The three component (ZNE) LH channel data (1 sample-per-second) were collected through Web site for *W* phase source inversions. We tested for six scenarios of two groups: group I using vertical component only and group II using all three ZNE components. In each group, three scenarios are tried with different level of knowledge on earthquake parameters: (1) using the GCMT centroid parameters (impractical in real events), (2) using the hypocenter parameters (lon., lat., depth, origin time) reported by the PDE catalogue, and a centroid time, t_c , determined by grid search; the source half duration, t_p , is set equal to t_c , (3) the same as (2) except the centroid location (lon., lat.) determined by a 2-dimensional grid search (depth fixed at PDE's). We indicate the three scenarios as gCMT location, t_c location, and $[t_c+xy]$ location, respectively. An example of final fitting between synthetic and observed waveforms of vertical component for the first shock of the M_w 7.0 Dec. 26, 2006, Pingtung earthquake is shown (Fig. 3). The frequency band used to filter seismic waveforms basically follows Table 1 of Hayes *et al.* [5] except that for a few $M_w \sim 6.0$ earthquakes, the band is fine-tuned to have better results.

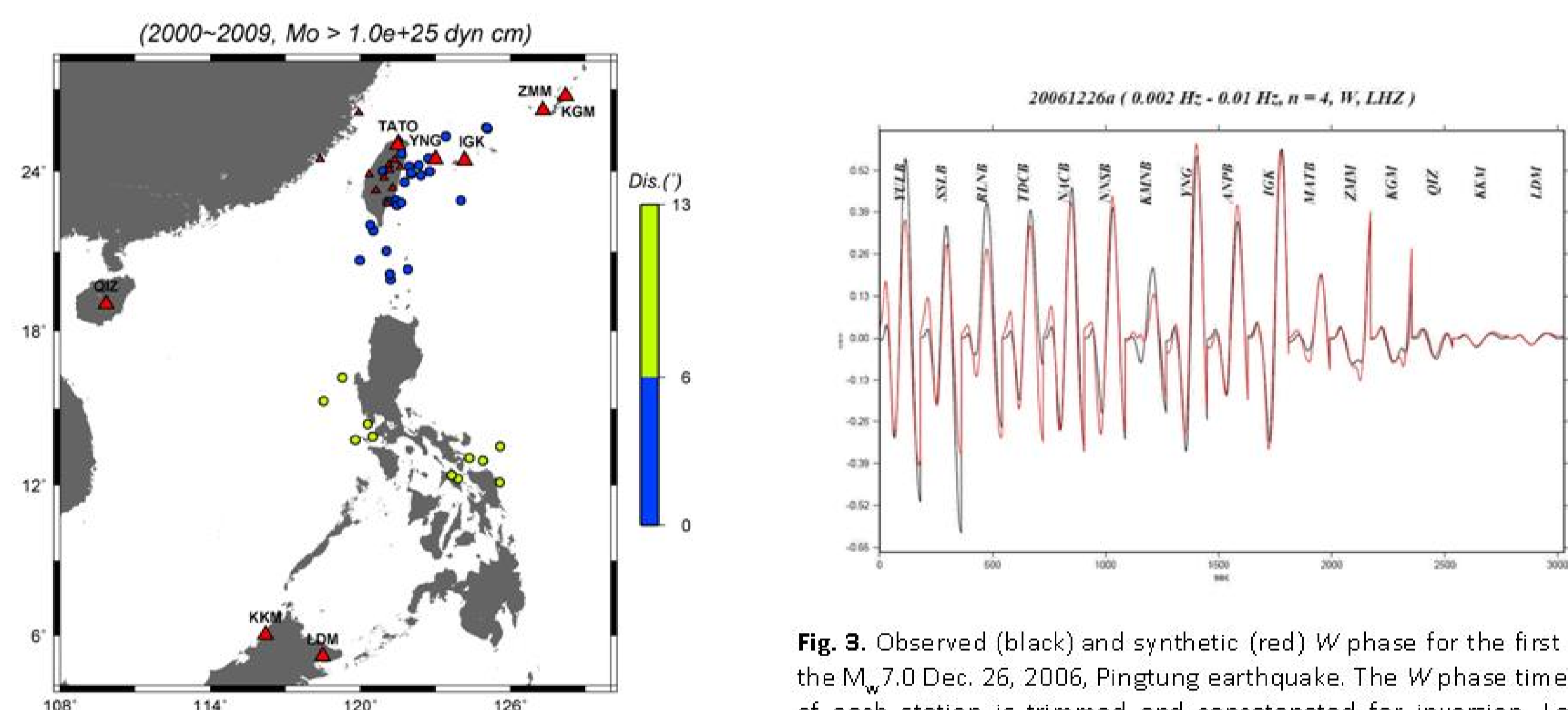


Fig. 3. Observed (black) and synthetic (red) *W* phase for the first shock of the M_w 7.0 Dec. 26, 2006, Pingtung earthquake. The *W* phase time window of each station is trimmed and concatenated for inversion. Labels are names of stations.

Fig. 2. Distribution of SCS earthquakes occurring from January 2000 to July 2009 (circles) with color-keyed epicentral distances relative to central Taiwan (blue for near group and green for far group). Triangles represent distribution of virtual network with non-BATS stations bigger symbol and labeled.

2.2. Unit Tsunami Methods

The unit tsunami methods pre-calculate propagation of unit sources with the resulting unit tsunamis stored in database for synthetics of real tsunami waves. The principle of unit tsunami methods is conceptually analogous to Green's function in Seismology and only works in linear systems. As compliance, we aim at predicting the offshore - prior to the run-up stage - arrival times and amplitudes of approaching tsunami waves, where the governed equations are the linear shallow water wave equations. The potential source region of the Manila subduction zone was divided into 14×10 square pixels, each with $0.5^\circ \times 0.5^\circ$ in size and an initial vertical seafloor displacement of 1 m was assigned to each pixel to constitute the group of unit sources (Fig. 4). We employed Cornell Multidimensional Coupled Tsunami Model (COMCOT; [6]) to simulate the propagations of each unit source. We set up 32 virtual stations representing existing tidal stations of Central Weather Bureau (Fig. 5). The wave field of one station from one unit source is referred to the unit tsunami corresponding to the station-unit source pair and the unit tsunamis for the 32 stations were stored in database. In the end, a total of $14 \times 10 \times 32$ unit tsunamis were stored in database for synthetics of tsunami waves in real events. The stored unit tsunamis are readily available for arrival time predictions even without the occurrence of real events. We applied Short Time Average over Long Time average (STA/LTA; [7]), a conventional scheme for picking seismic P and S phases, to automatically pick the arrival times of unit tsunamis with results stored in database for arrival time predictions.

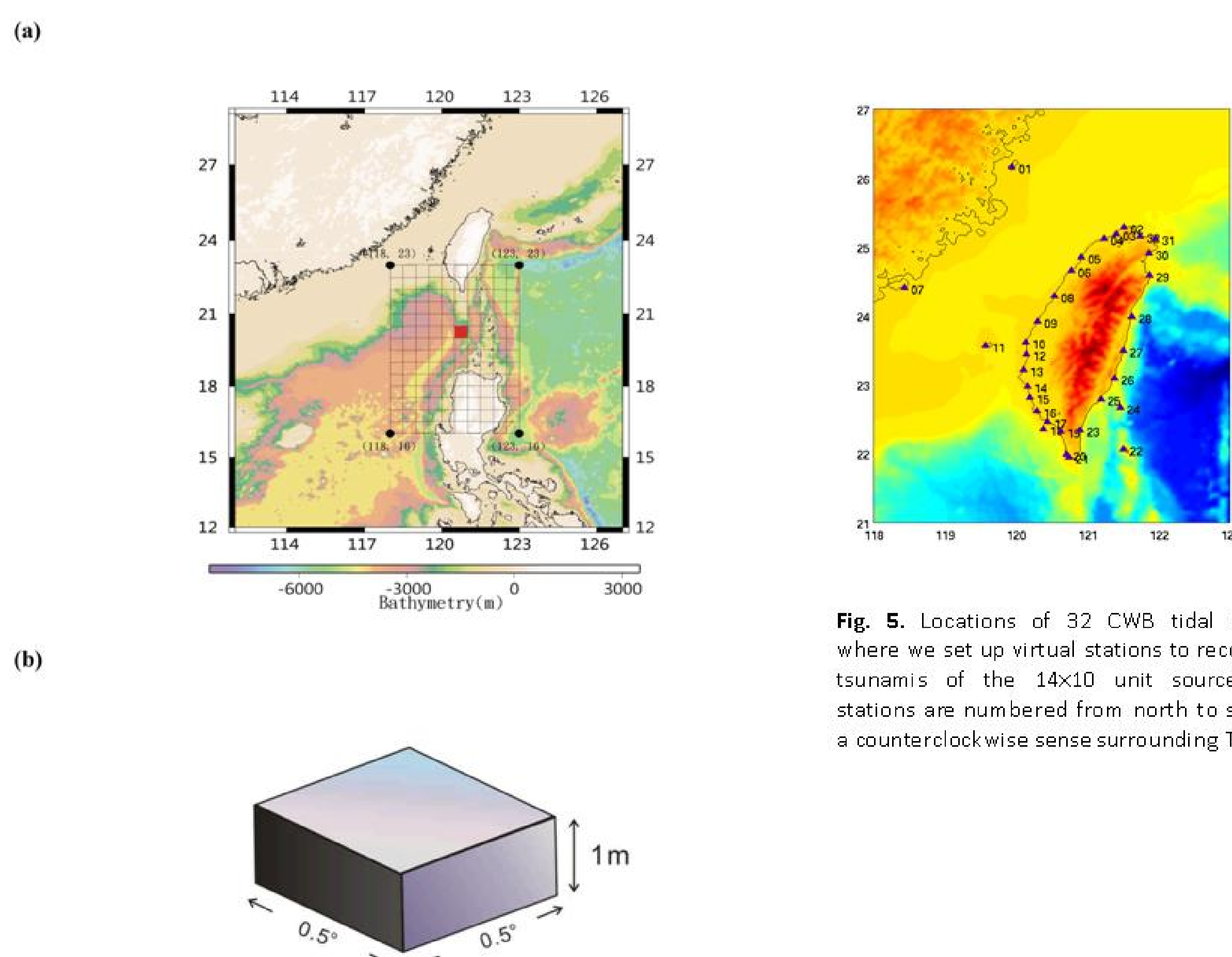


Fig. 5. Locations of 32 CWB tidal stations where we set up virtual stations to record unit tsunamis of the 14×10 unit sources. The stations are numbered from north to south in a counterclockwise sense surrounding Taiwan.

Fig. 4. (a) Division of the source region of the Manila subduction zone into 14 (latitudinal) times 10 (longitudinal) subregions of squares. The red pixel is the ninth from bottom and the sixth from left, indicated with 09_06. (b) The vertical displacement assigned to the pixel as unit source.

3. Results

3.1. W phase inversion

We judge the qualities of solutions based on the discrepancies between those of *W* phase inversion and those of GCMT solutions of the same event, in terms of both moment magnitudes (M_w) and focal mechanisms. The comparisons of M_w for six scenarios are presented in Fig. 6 with group I (Z component only) in the first column and group II (ZNE components) in the second column. The numbers in each box (scenario) indicate the absolute means of magnitude differences and corresponding standard deviations. The absolute means of all six scenarios are less than 0.1 unit, validating the application of *W* phase inversion using data of regional network to determine source parameters of SCS earthquakes greater than M_w 5.9. Among the three tried scenarios (gCMT location, t_c location, and $[t_c+xy]$ location), only the last two are practicable in real-time *W* phase inversion, among which the group II t_c location is the best scenario (least discrepancies). The Kagan rotation angle refers to the solid angle rotating from one double couple to another [8] and thus is a measurement of focal mechanism discrepancies. We present the Kagan angles - relative to the GCMT solutions of the same events - of the six scenarios in Figure 7 (ith mean and standard deviation indicated, using the same fashion as Figure 6). Again, the group II t_c location is the one with the minimum mean among all real-time practicable scenarios.

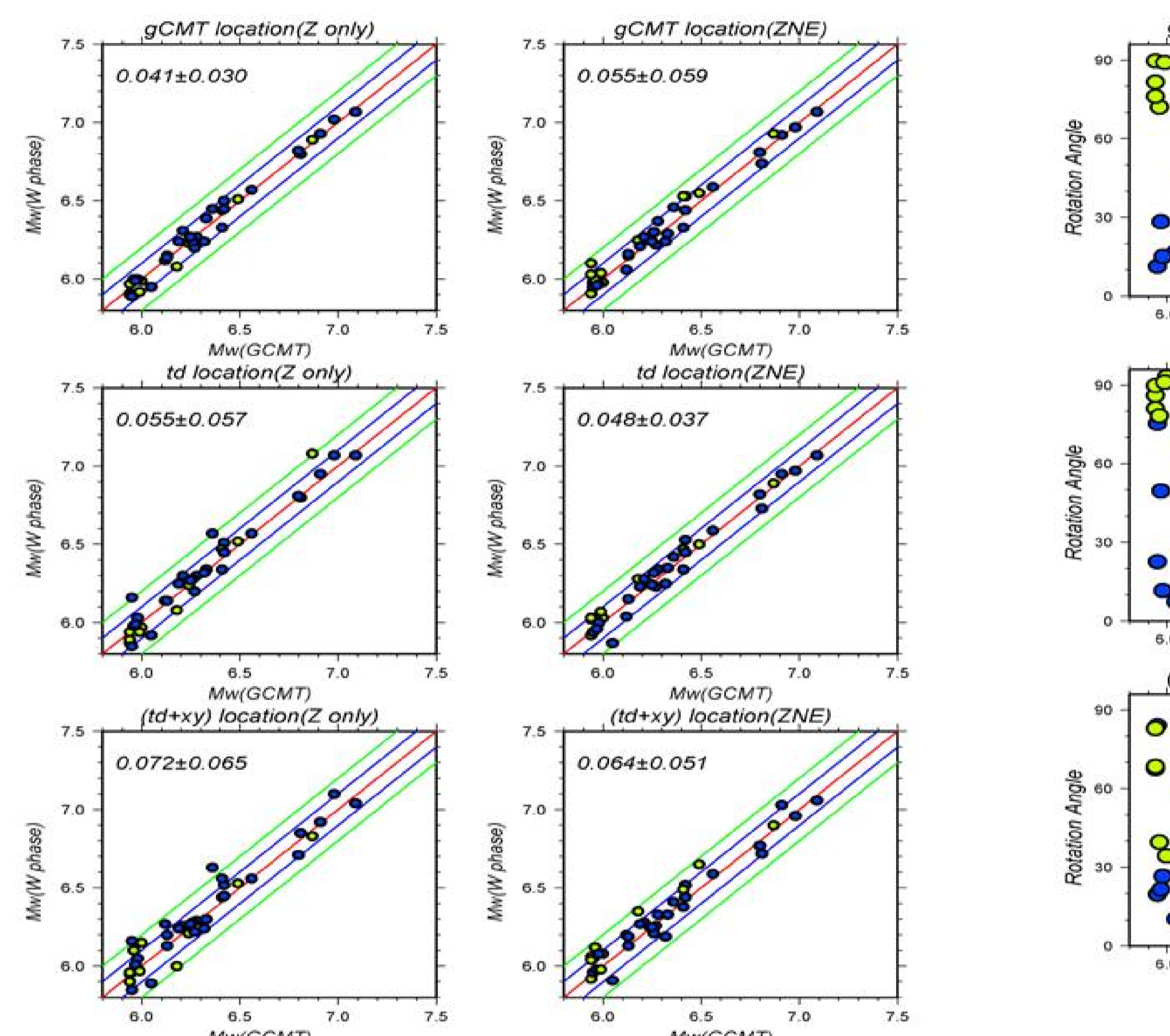


Fig. 6. Comparison of M_w (GCMT) and M_w (*W* phase) for earthquakes used in this study with blue for near group and green for far group. The left column is results of Z component only (group I) and the right one ZNE components (group II). Top to bottom represents three sets of scenario for different level of knowledge on earthquake parameters (see text). Numbers are mean values for differential M_w and standard deviation. The best result is those of group I GCMT location (top left) and the best one among practicable scenarios is group II t_c location.

Fig. 7. Rotation angle of source geometries between *W* phase and GCMT solutions, presented in the same fashion as Fig. 6. Again, the best result is those of group I GCMT location (top left) and the best one among practicable scenarios is group II t_c location.

3.2. Unit tsunamis

Characteristics of tsunami wave propagation in SCS and around Taiwan depend on bathymetric features and can be learned from simulated propagation of unit sources. Fig. 8 shows the propagation waves at different time frames of an exemplary unit source. Fig. 9a shows the resulting 32 unit tsunamis of the exemplary unit source, which demonstrate that stations 14 to 26 are the most affected ones with southern tip of Taiwan (stations 20, 21, and 23) being the most vulnerable (Fig. 5). The STA/LTA scheme works well in determining the arrival times of unit tsunamis (Fig. 9b) and we compile the data to produce one arrival-time map for each unit source (Fig. 10), which will also be stored in database and are readily for prompt arrival-time predictions.

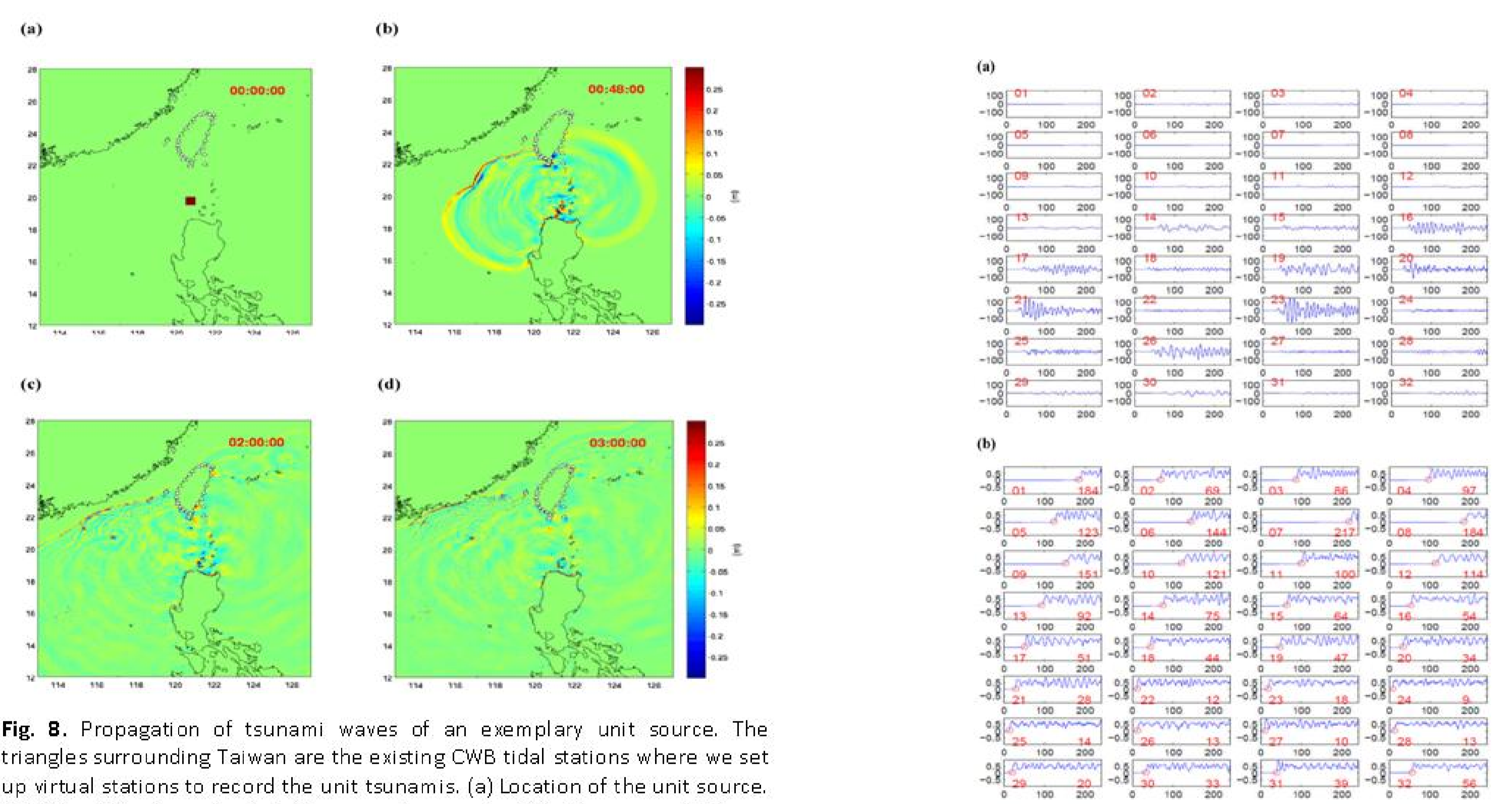


Fig. 8. Propagation of tsunami waves of an exemplary unit source. The triangles surrounding Taiwan are the existing CWB tidal stations where we set up virtual stations to record the unit tsunamis. (a) Location of the unit source. (b) After 48 min, note that the wave has reached Hualien on east Taiwan coast, but only Kaohsiung on that of western Taiwan due to significantly bathymetric differences. (c) At 2 hours, the tsunami wave along eastern Taiwan has reached the majority of north Taiwan and note that northwest Taiwan coasts have the most warning time. (d) After three hours, almost all Taiwan coasts have been attacked by tsunamis.

Fig. 9. (a) Unit tsunamis of the 32 virtual stations for the unit source in Fig. 8. Red numbers indicate stations following Fig. 5. Unit is minute for x-axis and cm for y-axis. (b) Results of STA/LTA scheme applying on the unit tsunamis. Note the sharp arrivals of tsunami waves make their picking robust. Unit is minute for x-axis and STA/LTA ratio for y-axis. The numbers to the right of each box is the picking arrival-time in minute.

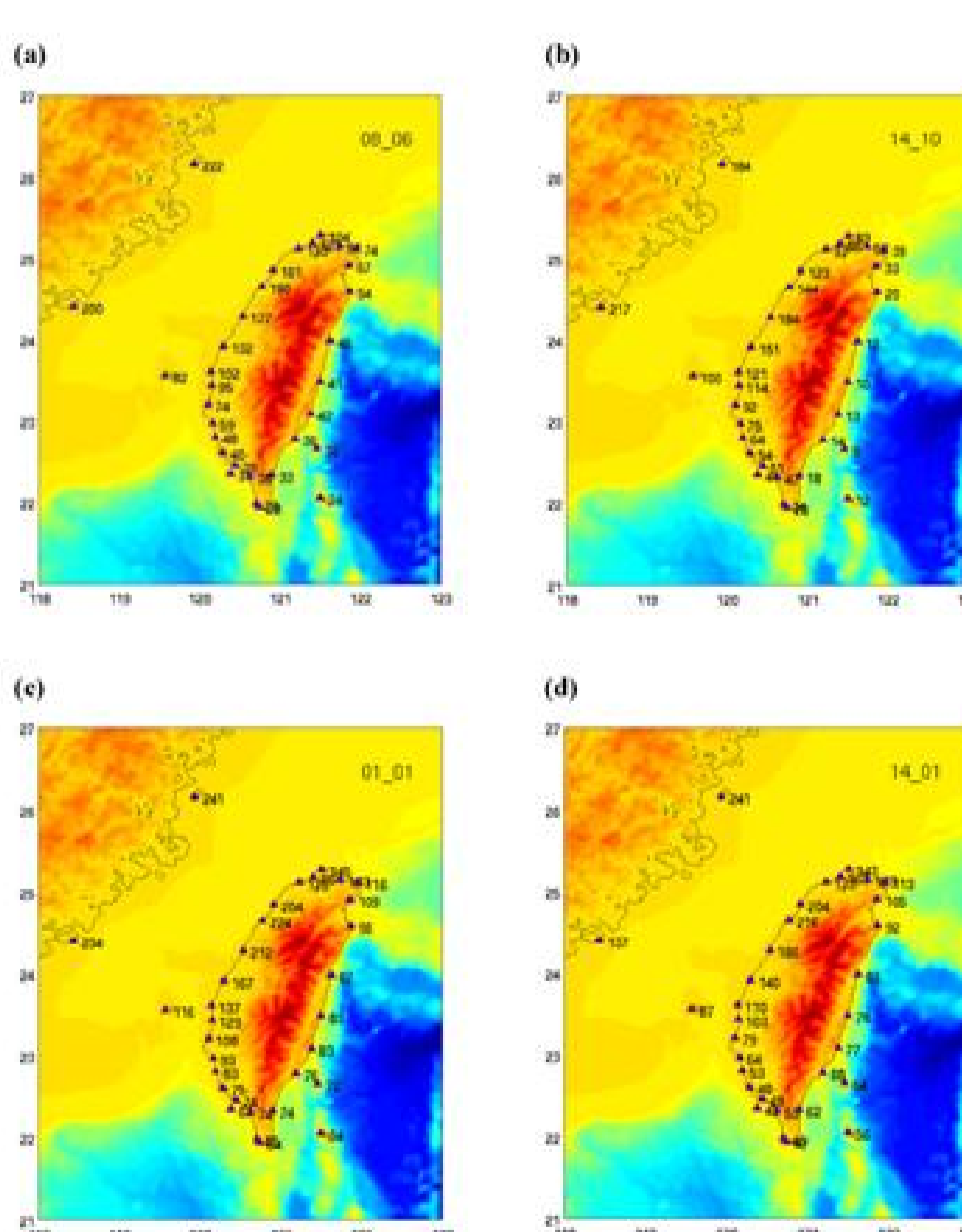


Fig. 10. The arrival time maps for different unit sources in minutes. See Figure 4 for nomenclature of unit source. (a) For the 08_06 unit source. (b) For the 14_10 unit source (the top right corner). (c) For the 01_01 unit source (the bottom left corner). (d) For the 14_01 unit source (the top left corner).

5. Conclusions

In this study, we propose to combine *W* phase inversion and unit tsunami methods to build a tsunami warning system in Taiwan for earthquakes in the SCS region. The *W* phase inversion allows us to rapidly determine moment tensors of large earthquakes for the calculations of vertical seafloor displacements. The applicability of *W* phase inversion for SCS earthquakes using BATS stations and its extension has been attested and expected to be improved, pending future completion of extended BATS. We have built a database of unit tsunamis for the source region of the Manila subduction zone and the prediction of arrival times is readily available once the epicenter of tsunamigenic earthquake is known.

- References
- [1] Soloviev S.L., Go Ch.N. Nauka Publishing House, Moscow, USSR, 310 pp., 1974. *Can. Transl. Fish. Aquat. Sci.* 5077, 1984.
 - [2] Kanamori H., Rivera L. *Geophys. J. Int.* 2008; 175: 222-238 doi: 10.1111/j.1365-246X.2008.03887.x
 - [3] Daswonski A.M., Chau T.A., Woodhouse J.H. *J. Geophys. Res.* 1981; 86: 2825-2832.
 - [4] Ekström G., Daswonski A.M., Mckenzie T.N., Nettles M. *Phys. Earth planet. Inter.* 2005; 148(1-2): 327-351.
 - [5] Hayes G.P., Rivera L., Kanamori H. *Seismological Research Letters* 2009; 80(5): 817-822 doi: 10.1785/gssrl80.5.817
 - [6] Liu P.L.-F., Woo S.-B., Cho Y.-S. Technical Report, Cornell University, 1998.
 - [7] Allen, R. *Bull. Seismol. Soc. Am.* 1982; 72(6): 225-242.
 - [8] Kagan, Y.Y. *Geophys. J. Int.* 1991; 106(3): 709-716.